

## Compensation and Improvement of Intensity and Distribution in Reconstructed Image Using Adaptive Optics in Holographic Data Storage

Tetsuhiko MUROI\*, Sayaka SEKIGUCHI<sup>1</sup>, Nobuhiro KINOSHITA, Norihiko ISHII, Naoki SHIMIDZU, Koji KAMIJO, Martin BOOTH<sup>2</sup>, Rimas JUSKAITIS<sup>2</sup>, and Tony WILSON<sup>2</sup>

*NHK Science and Technical Research Laboratories, 1-10-11 Kinuta, Setagaya-ku, Tokyo 157-8510, Japan*

<sup>1</sup>*Department of Materials Science and Engineering, Tokyo Denki University, 2-2 Kanda-Nishiki-cho, Chiyoda-ku, Tokyo 101-8457, Japan*

<sup>2</sup>*Department of Engineering Science, University of Oxford, Parks Road, Oxford OX1 3PJ, United Kingdom*

(Received November 30, 2007; accepted January 28, 2008; published online July 18, 2008)

We applied a genetic algorithm to adaptive optics to improve the intensity and distribution of reconstructed images in holographic data storage. This is a kind of combinatorial optimisation. In holographic data storage, the photopolymer recording medium shrinks during light curing and this shrinkage distorts the recorded interference fringes, which degrades the reconstructed data images. Although it is possible to compensate for the degradation in the reconstructed image by using adaptive optics, it has been difficult to compensate for the shrinkage distortion by using normal feedback control because the relationship between the reconstructed image and deformable mirror input is nonlinear. With our method, the inverse variance coefficient in a reconstructed image with bits that are all “1” increased from 10.3 to 14.7 dB, an improvement of 4.4 dB. Moreover, the intensity average of the reconstructed image with compensation was 1.7 times higher than the average without compensation. These results show that the combination of adaptive optics and a genetic algorithm is very effective for improving reconstructed images. [DOI: 10.1143/JJAP.47.5900]

KEYWORDS: holographic data storage, adaptive optics, compensation, genetic algorithm, wavefront

### 1. Introduction

Holographic data storage is expected for large-capacity and high-data-transfer-rate storage systems because data can be recorded three-dimensionally in a medium and a two-dimensional data array can be recorded and reproduced with parallel processing. One material that has been studied for the recording medium is photopolymer, which has a large diffraction efficiency and high stability.

A hologram is easily affected by the wavefronts of the signal and reference beams because it records amplitude and phase information of the beams. If a phase error between two beams occurs as a result of air disturbance during a recording, the maximum amplitude of interference fringes cannot be recorded on the medium. Adaptive optics<sup>1,2)</sup> is very effective at compensating for the phase error, and it may be applied to a holographic data storage system while recording.<sup>3,4)</sup>

On the other hand, the photopolymer medium shrinks as a result of photopolymerization when holograms are recorded in it. Moreover, a temperature difference between the recording and reconstructing conditions causes the photopolymer to shrink or expand,<sup>5,6)</sup> distorting the recorded interference fringes. If there were no distortion in the recording medium, the wavefront of the reconstructed beam would be the same as that of the signal beam. In contrast, if distortion caused by shrinkage or temperature change does occur, the reconstructed beam will have a distorted wavefront. Subsequently, reconstructed data pages would show a lower signal-to-noise ratio (SNR). In this paper, we describe the use of adaptive optics to compensate for degradation of a reconstructed beam caused by medium shrinkage or temperature change. The intensity and distribution in reconstructed images are improved.

### 2. Optical Configuration and Recording/Reconstruction of Hologram

#### 2.1 Optical configuration for adaptive optics

The optical configuration for holographic data storage using adaptive optics is shown in Fig. 1. A laser beam is divided into signal and reference beams by a polarized beam splitter (PBS). The reference beam reaches the medium through a deformable mirror (DM) for adaptive optics. A cross-sectional view and top image of the DM are shown in Fig. 2. The DM has 19 pins and there is a thin mirror on each pin. Each pin can be controlled independently. Therefore, any type of wavefront can be produced. Furthermore, lenses A between the PBS and the DM and lenses B between the beam splitter (BS) and medium are set in the path of the reference beam. Lenses A are set to compensate for the initial defocusing of the DM. Lenses B are set to demagnify the diameter of the reference beam reflected by the DM. The reconstructed beam is observed with a Shack Hartmann wavefront sensor (SHWS), which measures the wavefront and intensity distribution of the reconstructed beam. The SHWS and the DM are connected to a personal computer (PC). The SHWS measures the intensity and phase of the reconstructed beam, and the PC controls the DM to compensate for the reference beam entering the hologram.

#### 2.2 Recording/reconstruction without compensation

In the optical configuration in Fig. 1, the interference fringes between the signal beam carrying information about a data page with data bits that are all “1” and the reference beam were recorded in a photopolymer medium as a hologram. The recording medium that we used consisted of two types of monomers;<sup>7)</sup> i.e., M-110 and M-1600 (Toa Gosei). After a hologram had been recorded, the reference beam was irradiated onto the hologram, and a reconstructed image of the data page was obtained. The reconstructed image without compensation is shown in Fig. 3(a). A uniform white image was expected because the recorded

\*E-mail address: muroi.t-hc@nhk.or.jp

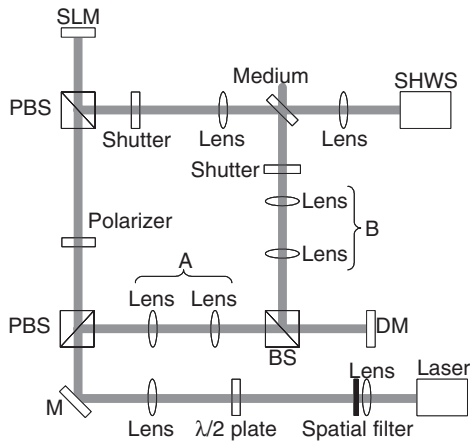


Fig. 1. Optical configuration for holographic data storage using adaptive optics.

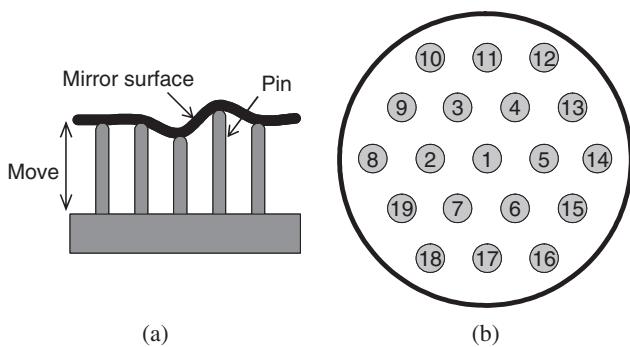


Fig. 2. Concept of deformable mirror: (a) cross sectional view and (b) top image.

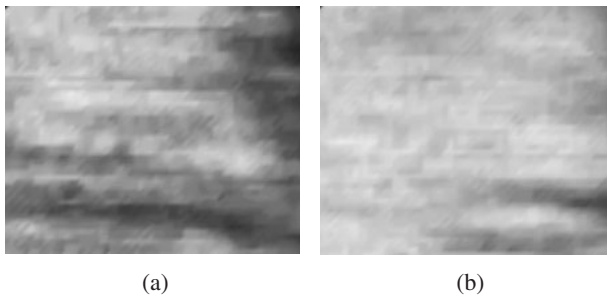


Fig. 3. Image reconstructed from hologram: (a) without compensation and (b) with compensation.

data bits were all “1”. However, several areas are dark, and a large intensity distribution can be seen because the interference fringes experienced shrinkage while the medium was being cured.

### 3. Control Method for Improving Intensity and Distribution

#### 3.1 Control DM using transfer function

In adaptive optics with a DM and SHWS, the most popular control method is a feedback control system using a transfer function.<sup>8)</sup> We tested the use of this method with the DM pin’s values as input and Zernike polynomials of the beam as output. In this study, Zernike polynomials were defined as shown in Table I, i.e., the first and second

Table I. Zernike polynomials.

Order	Equation	Aberration
1	$\rho \cos(\theta)$	Tilt at 0°
2	$\rho \sin(\theta)$	Tilt at 90°
3	$2\rho^2 - 1$	Focus
4	$\rho^2 \cos(2\theta)$	Astigmatism 0°
5	$\rho^2 \sin(2\theta)$	Astigmatism 45°

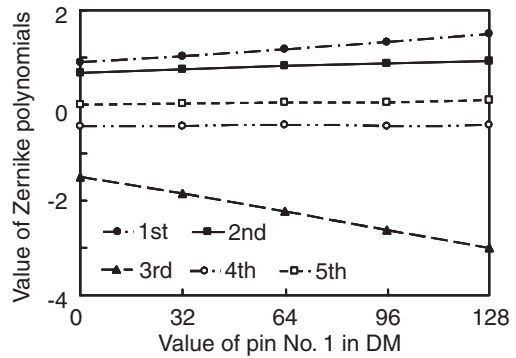


Fig. 4. Values of Zernike polynomials in the reference beam as a function of the value of pin No. 1 in the DM.

orders were tilt, third order was focus, fourth and fifth order were astigmatism, and so on. First, we confirmed the linearity of the static response between the DM values and Zernike polynomials of the reference beam. In this investigation, the holographic recording medium was not included. Figure 4 shows the values of the first to fifth order Zernike polynomials as a function of the value of pin No. 1 in the DM, as shown in Fig. 2(b). All order values were linear with respect to the pin’s value. Therefore, the relation between the DM values and Zernike polynomial can be expressed as

$$Z = AD. \tag{1}$$

Here,  $D$  is composed of the DM values, which are represented by

$$D = \begin{pmatrix} d_1 \\ d_2 \\ d_3 \\ \vdots \\ d_n \end{pmatrix}, \tag{2}$$

where  $d_n$  is the value of pin  $n$ .  $Z$  is the Zernike polynomials, which are represented by

$$Z = \begin{pmatrix} z_1 \\ z_2 \\ z_3 \\ \vdots \\ z_m \end{pmatrix}, \tag{3}$$

where  $z_m$  is the value of the  $m$ -th order Zernike polynomial.  $A$  is the proportionality constant matrix, which is represented by

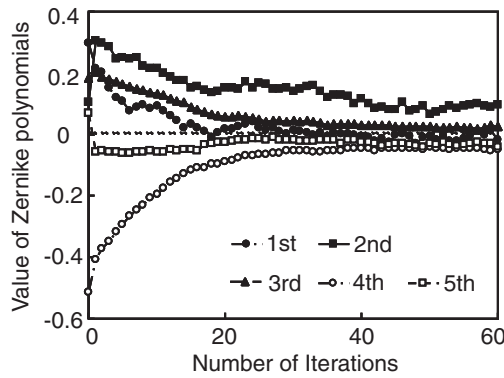


Fig. 5. Values of Zernike polynomials in the reference beam as a function of the number of iterations.

$$A = \begin{pmatrix} a_{11} & a_{12} & a_{13} & \cdots & a_{1n} \\ a_{21} & \ddots & & & \vdots \\ a_{31} & & \ddots & & \vdots \\ \vdots & & & \ddots & \vdots \\ a_{m1} & \cdots & \cdots & \cdots & a_{mn} \end{pmatrix}, \quad (4)$$

where  $a_{mn}$  is the proportionality constant of  $z_m$  and  $d_n$ . Then, feedback control can be carried out using

$$D_{k+1} = \beta A^{-1}(Z_{\text{req}} - Z_k) + D_k. \quad (5)$$

Here,  $D_k$  is the  $k$ -th DM value,  $Z_k$  is the measured value of the Zernike polynomial under the condition of  $D_k$ ,  $Z_{\text{req}}$  is the required Zernike polynomial, and  $\beta$  is a constant. This indicates that the reference beam can be controlled by using feedback when inverse  $A$  exists. The measured values of Zernike polynomials as a function of iteration  $k$  are shown in Fig. 5. When the values of all order Zernike polynomials are zero, a flat wavefront can be obtained. Therefore, in this experiment,  $Z_{\text{req}}$  was set to

$$Z_{\text{req}} = \begin{pmatrix} 0 \\ 0 \\ 0 \\ \vdots \\ 0 \end{pmatrix}. \quad (6)$$

As shown in Fig. 5, all order values approached zero, which indicates that the feedback control certainly worked.

Next, we investigated the relationship between the DM values and Zernike polynomials of the reconstructed beam diffracted by the photopolymer medium where the interference fringes were recorded. Values of the first to fifth order Zernike polynomials as a function of the value of pin No. 1 in the DM are shown in Fig. 6. The values of the Zernike polynomials are not linear with respect to the pin value. This is why photopolymer shrinkage occurred nonuniformly in the irradiated area. This suggests that the distribution of distortion in the recorded interference fringes would depend on how shrinkage occurred in the recording medium. Therefore, the reconstructed beam from this interference fringe was nonlinear with respect to the DM values. As a result, the transfer function was complex, and it was difficult to control the wavefront of the reconstructed beam using normal feedback control.

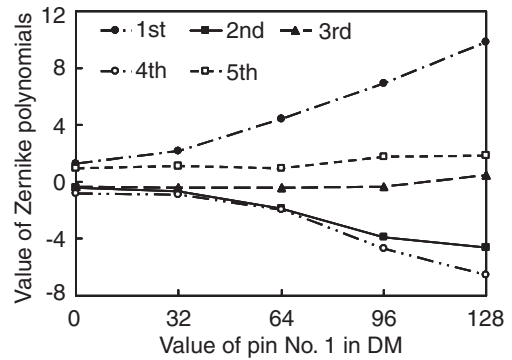


Fig. 6. Values of Zernike polynomials in the reconstructed beam as a function of the value of pin No. 1 in the DM.

### 3.2 Controlling the DM using a genetic algorithm

In the previous section, we showed that it was difficult to compensate for degradation of the reconstructed beam with feedback control using the transfer function. Therefore, we tried using combinatorial optimisation. There are two types of combinatorial optimisation: exact analysis and approximate analysis.<sup>9)</sup> With exact analysis, the reconstructed beams must be measured under all DM conditions to obtain an optimised condition. Consequently, this analysis is not suitable for fast compensation. On the other hand, there are several methods for approximate analysis. The Monte-Carlo method can give high accuracy but is not very fast. The iterative improvement method can compensate quickly but not very accurately. The genetic algorithm (GA) can compensate both accurately and quickly, so we chose to use a GA to compensate for degradation of the reconstructed beam for adaptive optics.

The parameters used in the GA are gene, individual, population, and fitness. The genes are defined as the values of the pins driving the DM. The individual is the condition of the DM as determined by genes. The population is a group of  $s$  individuals. The fitness is an evaluation parameter, which represents how well the individual fits the environment. It is defined as the inverse of the variation coefficient (IVC) in a reconstructed image in which all data bits are “1”, i.e., a white image. IVC is represented by

$$\text{IVC} = 20 \log \frac{\mu}{\sigma}, \quad (7)$$

where  $\mu$  and  $\sigma$  represent mean and standard deviation of intensity in the reconstructed image, respectively. IVC was used instead of the variation coefficient for consistency with the SNR. The GA was executed to obtain the maximum IVC.

The flow chart of the GA is shown in Fig. 7. First, we have a  $k$ -th generation population  $P_k$ , which consists of  $s$  individuals. Each value for the DM's pins of individuals in the initial population  $P_0$  is determined randomly. The first operations are reproduction and crossover. In crossover, two individuals are selected from the population and a crossover point is randomly defined. For example, let us consider that the crossover is for individuals  $X$  and  $Y$ , and the crossover point is between pins  $p$  and  $p + 1$ . The value for pin numbers less than  $p$  for individual  $X$  and for pin numbers greater than  $p + 1$  for individual  $Y$  are mixed, resulting in individual  $X'$ .

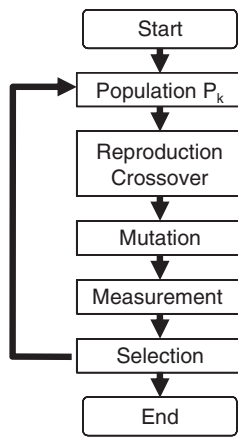


Fig. 7. Flow chart for genetic algorithm used in adaptive optics.

Likewise, the value for pin numbers greater than  $p + 1$  for individual  $X$  and for pin number less than  $p$  for individual  $Y$  are mixed, resulting in individual  $Y'$ . As a result, two new individuals are generated. This crossover is applied to all individuals. The second operation is mutation. An individual is selected with probability  $F_m$ . For the selected individual, the value of the randomly selected pin is changed randomly. After that, for each individual, the DM values are set, the reconstructed images are measured with the SHWS, and IVC is calculated. Finally,  $s$  individuals with higher IVC values are selected, and they form the next-generation population,  $P_{k+1}$ . By repeating this process, generation alternation is achieved, and a higher IVC can be obtained.

#### 4. Improvement of Intensity Distribution in Reconstructed Image

We compensated for the degradation of the reconstructed image shown in Fig. 3(a) by using adaptive optics with the GA described in the previous section. We tried to improve the IVC in a reconstructed image by changing the wavefront of the reference beam by means of the DM. The GA conditions were as follows: the number of individuals in population  $s$  was 20, generation alternation  $k$  was 50, and mutation probability  $F_m$  was 0.1. In this experiment, the area measured with the SHWS in the reconstructed image was a circle with a diameter of 10 mm. IVC is shown as a function of the generation alternation in Fig. 8. The solid and dotted lines show the highest and mean IVCs in the population  $P_k$ . As shown in Fig. 8, IVC increased up to the 28th generation but then decreased between the 28th and 38th generations. We considered possible reasons as follows. One possibility is that mutation occurred at the individual having the highest IVC value. Another is that the medium temperature changed during measurement, which would have changed the distortion of the interference fringe. However, IVC increased again after the 38th generation. We think that the GA searched for a new optimum DM condition. Then, it can be assumed that the IVC value saturated after the 20th generation. IVC without compensation was 10.3 dB and after 50 generations was 14.7 dB. Accordingly, IVC was improved by 4.4 dB. The reconstructed image with compensation is shown in Fig. 3(b). We found that the uniformity of the image was improved. Furthermore, the average intensity with compensation was 1.7 times higher than without compensa-

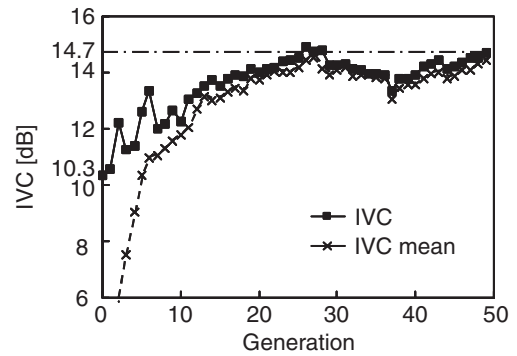


Fig. 8. Improved inverse variation coefficient obtained by using adaptive optics with a genetic algorithm.

tion. In this experiment, compensation took considerable time because the response time of the DM with a piezo-actuator was slow. If a phase modulator such as a liquid crystal device were used, fast compensation should be achievable. Adaptive optics with the GA can adequately find the wavefront conditions of the reference beam required to compensate for medium shrinkage and improve the IVC of a reconstructed image.

#### 5. Conclusions

In holographic data storage, the photopolymer medium shrinks due to irradiation of the laser beam, which causes distortion of the recorded interference fringes. This distortion degrades the reconstructed image. We described a method of compensating for the degradation in the reconstructed images by controlling the wavefront of the reference beam. We found that the relationship between the reconstructed image and the DM input values was nonlinear and that feedback control was difficult. Therefore, we used adaptive optics with a genetic algorithm. In an experiment on reconstructing an image with bits that were all "1", the inverse variation coefficient, which is related to the signal-to-noise ratio, increased from 10.3 to 14.7 dB. Moreover, the intensity average of the reconstructed image with compensation was 1.7 times higher than the average without compensation. The combination of adaptive optics and a genetic algorithm is useful for improving the reconstructed image. Furthermore, this technology is promising for reconstructing random bit data.

- 1) M. Booth, M. Neil, R. Juskaitis, and T. Wilson: *Proc. Natl. Acad. Sci. U.S.A.* **99** (2002) 5788.
- 2) M. Booth, T. Wilson, H. Sun, T. Ota, and S. Kawata: *Appl. Opt.* **44** (2005) 5131.
- 3) N. Ishii, N. Kinoshita, T. Muroi, K. Kamijo, and N. Shimidzu: *Jpn. J. Appl. Phys.* **46** (2007) 3862.
- 4) N. Ishii, T. Muroi, N. Kinoshita, K. Kamijo, and N. Shimidzu: *Proc. SPIE* **6488** (2007) 64880G.
- 5) S. Baba, S. Yoshimura, and N. Kihara: *Jpn. J. Appl. Phys.* **45** (2006) 1258.
- 6) M. Toishi, A. Fukumoto, and K. Watanabe: *IWHM '07 Dig.*, 2007, 27p02.
- 7) M. L. Schilling, V. L. Colvin, L. Dhar, A. L. Harris, F. C. Schilling, H. E. Katz, T. Wysocki, A. Hale, L. L. Blyler, and C. Boyd: *Chem. Mater.* **11** (1999) 247.
- 8) E. J. Fernandez and P. Artal: *Opt. Express* **11** (2003) 1056.
- 9) N. Sannomia, H. Kita, H. Tamaki, and T. Iwamoto: *Iden Arugorizumu to Saitekika* (Genetic Algorithms and Optimization) (Asakura, Tokyo, 2004) pp. 9–11 [in Japanese].